

A Multi-Line De-Embedding Technique for mm-Wave CMOS Circuits

Naoki Takayama, Kouta Matsushita, Shogo Ito, Ning Li, Keigo Bunsen,
Kenichi Okada, and Akira Matsuzawa

*Department of Physical Electronics, Tokyo Institute of Technology
2-12-1 S3-27 Ookayama, Meguro-ku, Tokyo 152-8552 Japan
takayama@ssc.pe.titech.ac.jp*

Abstract—This paper proposes a de-embedding method for on-chip S-parameter measurements at mm-wave frequency. The proposed method uses only two transmission lines with different length. In the proposed method, a parasitic-component model extracted from two transmission lines can be used for de-embedding for other-type DUTs like transistor, capacitor, inductor, etc. The experimental results show that the error in characteristic impedance between the different-length transmission lines is less than $1\ \Omega$.

Index Terms—De-embedding, S-parameter measurement, mm-wave, RF CMOS, Transmission Line.

I. INTRODUCTION

Recently, the research on mm-wave CMOS circuits becomes a hot topic [1], [2]. CMOS process is employed for developing mm-wave wireless systems because of the low cost fabrication comparing with compound semiconductors [3]. In mm-wave circuits, even small parasitic capacitors and inductors will enormously affect the total circuit performance. Therefore, it is needed to build accurate models of the components including parasitic elements, such as transistors, capacitor, transmission-line, and so on.

Before building them, the process, de-embedding, is needed to remove parasitic components from measurement data because measurement data include the parasitic components of the contact pads. A variety of de-embedding methods for on-chip measurement have been proposed [4], [5]. There is one of the most common method called open-short method [6]. The method, however, cannot remove parasitic components of the contact pads completely in high frequency because it is difficult to fabricate an ideal short dummy pattern.

Some de-embedding methods using only line dummy patterns without short dummy pattern were proposed [7], [8], [9]. One of them uses a thru dummy pattern [7]. However, the measurement result of the thru dummy pattern has a large uncertainty and is not reliable because the value of the S-parameter is too small. Thus, the de-embedding result is also not reliable. The de-embedding method using only long line dummy patterns is proposed in [8]. However, this method considers only the parallel parasitic component of the contact pads and the series parasitic component are ignored. Moreover, this method is only applicable to de-embedding of a transmission line, not for other test element groups. In addition, there is a de-embedding method using two transmission lines that the length of the one is two times longer than that of the other [9].

The new technique proposed in this paper can remove not only the parallel parasitic components of the pads but also

the series one by using two transmission lines with different length. In addition, this method can be applied to other test element groups, such as transistors, capacitors, and so on, by building a model of the contact pads.

II. CONVENTIONAL METHODS

A. Open-Short De-embedding

At first, we introduce Open-Short De-embedding noted above [6]. This method builds the model of the contact pads and the ground plane, as shown in Fig. 1, from the measurement data of an open dummy pattern and a short dummy pattern. The equivalent circuits of the dummy patterns are shown in Fig. 2. The parallel parasitic components (Y_{P1} , Y_{P2} , Y_{P3}) are removed from the measurement data by subtracting the Y-parameter of the open dummy pattern. As the same procedure, the parallel parasitic components of a short pattern can be removed. Therefore, the matrix consisting of only series parasitic components (Z_{S1} , Z_{S2} , Z_{S3}) is obtained. By subtracting this matrix, the matrix of the DUT is obtained.

However this method has an issue at high frequencies like mm-wave frequency. It is impossible to fabricate ideal open and short patterns due to parasitic capacitance and inductance,

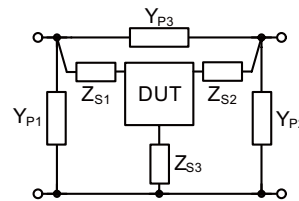


Fig. 1. Equivalent circuit used in the open-short de-embedding.

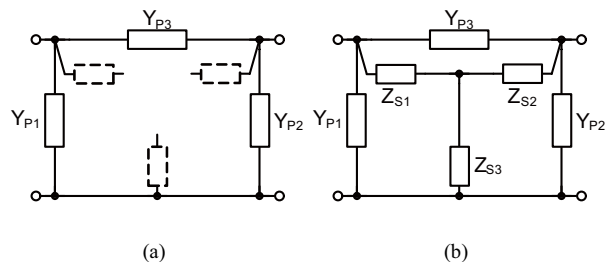


Fig. 2. Equivalent circuits. (a) Open dummy pattern. (b) Short dummy pattern.

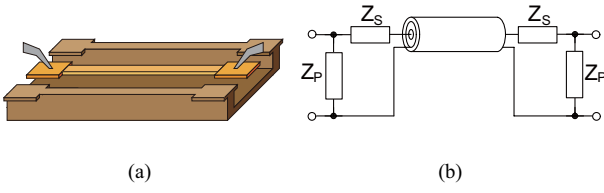


Fig. 3. Transmission line. (a) Structure. (b) Equivalent circuit.

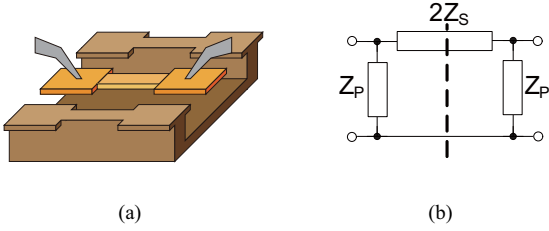


Fig. 4. Short thru. (a) Structure. (b) Equivalent circuit.

and the nonideality causes considerable degradation in the de-embedding accuracy, especially at the mm-wave frequency.

B. Thru-Only De-Embedding

Next, we introduce the thru-only de-embedding [7]. Fig. 3 shows the structure of a transmission line and the equivalent circuit of the measurement data. This method uses only a short thru dummy pattern. Fig. 4 shows the structure of a short thru and the equivalent circuit. The π -type equivalent circuit is utilized to characterize the measurement data. The pad model is built by separating the equivalent circuit into two symmetric parts.

However, this method has an issue. The length of the short thru has to be as short as possible because the equivalent circuit consists of lumped components. However, if the length is short, the distance between the probes is too close. Therefore, the measurement data become poorly-reproducible and unreliable.

III. PROPOSED METHOD

A. Multi-Line De-Embedding

As explained in the previous sections, the conventional open-short and thru-only methods are not so accurate at mm-wave frequencies, which is caused by the nonideality of open- and short-patterns and the inaccuracy of the short thru pattern. Thus, this paper proposes a novel de-embedding method using two long line patterns. In this method, first the transmission line is characterized by using the measurement data. The parasitic components of the contact pads are calculated and the pad model is built. The pad model built by two transmission lines can be utilized to de-embed the pad parasitics of other-type DUTs such as transistors, capacitors, inductors, etc. The procedure of the proposed method is as follows.

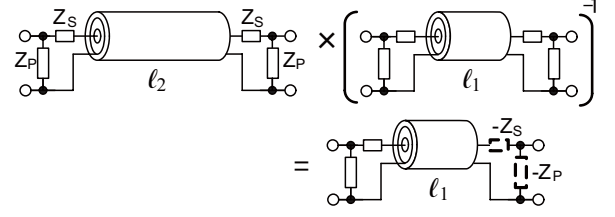


Fig. 5. Multiplying the matrixes of the transmission line.

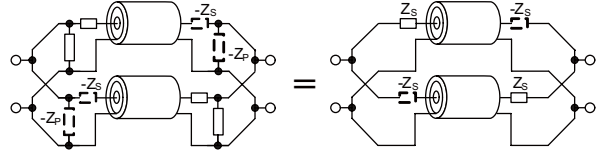


Fig. 6. Canceling the pad parasitic Z_P .

B. De-Embedding Procedure

Before building the model of the contact pads, the transmission line has to be characterized. Measurement data of two transmission lines with a length of ℓ_1 and ℓ_2 , where $\ell_2 = 2\ell_1$, are used in this method. Separating the segments of contact pads from the intrinsic line, the T-parameter matrix of test structure ℓ_i , $\mathbf{T}_{\ell_i}^m$, can be expressed by the following equation.

$$\mathbf{T}_{\ell_i}^m = \mathbf{T}_{PL} \cdot \mathbf{T}_{\ell_i} \cdot \mathbf{T}_{PR}, \quad (1)$$

where

\mathbf{T}_{ℓ_i} represents the T-parameter of the intrinsic line ℓ_i , \mathbf{T}_{PL} represents the T-parameter of the left pad, and \mathbf{T}_{PR} represents the T-parameter of the right pad.

Subsequently \mathbf{T}_{X1} is defined as multiplying $\mathbf{T}_{\ell_2}^m$ by the inverse of $\mathbf{T}_{\ell_1}^m$ (Fig. 5).

$$\begin{aligned} \mathbf{T}_{X1} &= \mathbf{T}_{\ell_2}^m \cdot [\mathbf{T}_{\ell_1}^m]^{-1} \\ &= \mathbf{T}_{PL} \cdot \mathbf{T}_{\ell_2} \cdot \mathbf{T}_{PR} \cdot \mathbf{T}_{PR}^{-1} \cdot \mathbf{T}_{\ell_1}^{-1} \cdot \mathbf{T}_{PL}^{-1} \\ &= \mathbf{T}_{PL} \cdot \mathbf{T}_{\ell_1} \cdot \mathbf{T}_{PL}^{-1} \end{aligned} \quad (2)$$

T-parameter of this matrix \mathbf{T}_{X1} is transformed to the Y-parameter matrix \mathbf{Y}_{X1} . A parallel combination of \mathbf{Y}_{X1} and a port-swapped version of itself, $\text{Swap}(\mathbf{Y}_{X1})$, is defined as \mathbf{Y}_{X2} . Thus, we can cancel the effect of the pad parasitic Z_P as shown in Fig. 6.

$$\begin{aligned} \mathbf{Y}_{X2} &= \mathbf{Y}_{X1} + \text{Swap}(\mathbf{Y}_{X1}) \\ &= \begin{bmatrix} Y_{X1_{11}} & Y_{X1_{12}} \\ Y_{X1_{21}} & Y_{X1_{22}} \end{bmatrix} + \begin{bmatrix} Y_{X1_{22}} & Y_{X1_{21}} \\ Y_{X1_{12}} & Y_{X1_{11}} \end{bmatrix} \end{aligned} \quad (3)$$

\mathbf{Y}_{X3} is defined as the Y-parameter matrix of the intrinsic TL connected with the pad series parasitic component Z_S and the negative parameter of itself $-Z_S$. Fig. 7 shows the equivalent circuit of \mathbf{Y}_{X3} . Assuming the structure of the intrinsic TL is perfectly symmetric, the Y-matrix of the intrinsic TL can be

expressed by Eq. (4). By using Eq. (6), \mathbf{Y}_{X3} is approximated by Eq. (5).

$$\mathbf{Y}_{TL} = \begin{bmatrix} Y_{TL-1} & Y_{TL-2} \\ Y_{TL-2} & Y_{TL-1} \end{bmatrix} \quad (4)$$

$$\mathbf{Y}_{X3} \simeq \begin{bmatrix} Y_{TL-1} - \frac{Z_S}{\Delta Z^2} & Y_{TL-2} \\ Y_{TL-2} & Y_{TL-1} + \frac{Z_S}{\Delta Z^2} \end{bmatrix} \quad (5)$$

$$\Delta Z^2 = \frac{1}{Y_{TL-1}^2 - Y_{TL-2}^2} - Z_S^2 \simeq \frac{1}{Y_{TL-1}^2 - Y_{TL-2}^2} \quad (6)$$

Therefore, \mathbf{Y}_{X2} can be obtained as the twofold of \mathbf{Y}_{TL} as explained in Eq. (7). By the procedure as mentioned above, the Y-parameter matrix of the intrinsic TL \mathbf{Y}_{TL} is obtained.

$$\begin{aligned} \mathbf{Y}_{X2} &= \mathbf{Y}_{X3} + \text{Swap}(\mathbf{Y}_{X3}) \\ &= \begin{bmatrix} 2Y_{TL-1} & 2Y_{TL-2} \\ 2Y_{TL-2} & 2Y_{TL-1} \end{bmatrix} = 2\mathbf{Y}_{TL} \end{aligned} \quad (7)$$

For de-embedding of other DUTs such as transistors, capacitors, inductors, etc, the pad parasitics of Z_S and Z_P are derived, which are frequency-dependent parameters. The Y-parameter matrix of the measurement data, \mathbf{Y}_{TL}^m , of the TL is expressed by \mathbf{Y}_{TL} in Eq. (8).

$$\mathbf{Y}_{TL}^m = \begin{bmatrix} \frac{Z_S + Z'_1}{\Delta Z'^2} + \frac{1}{Z_P} & \frac{Z'_2}{\Delta Z'^2} \\ \frac{Z'_2}{\Delta Z'^2} & \frac{Z_S + Z'_1}{\Delta Z'^2} + \frac{1}{Z_P} \end{bmatrix} \quad (8)$$

$$\Delta Z'^2 = (Z_S + Z'_1)^2 - Z'_2^2$$

$$Z'_1 = \frac{Y_{TL-1}}{Y_{TL-1}^2 - Y_{TL-2}^2}, \quad Z'_2 = \frac{Y_{TL-2}}{Y_{TL-1}^2 - Y_{TL-2}^2}$$

The Y-parameter matrix \mathbf{Y}_{X4} is defined as expressed in Eq. (9). If Eq. (11) is satisfied, the parallel parasitic Z_P is obtained by adding $Y(1,1)$ and $Y(1,2)$ of \mathbf{Y}_{X4} as expressed in Eq. (10).

$$\mathbf{Y}_{X4} = \mathbf{Y}_{TL}^m - \mathbf{Y}_{TL} \quad (9)$$

$$Y_{X4-11} + Y_{X4-12} \simeq \frac{1}{Z_P} \quad (10)$$

$$\left| \frac{1}{Z_P \cdot (Y_{TL-1} + Y_{TL-2})} \cdot \left(1 + \frac{1}{Z_S \cdot (Y_{TL-1} + Y_{TL-2})} \right) \right| \gg 1 \quad (11)$$

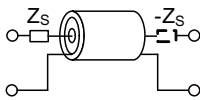


Fig. 7. The equivalent circuit of \mathbf{Y}_{X3} .

Next, we evaluate the pad series parasitic component Z_S . By subtracting the parallel parasitics from the measurement data of the TL, we can obtain \mathbf{Y}_{X5} that is the parameter of the intrinsic TL with the series parasitic components as expressed in Eq. (12). Then we calculate the resistance and inductance of this parameter as shown in Fig. 8. This procedure is implemented by using two transmission lines with different length.

$$\mathbf{Y}_{X5} = \mathbf{Y}_{TL}^m - \begin{bmatrix} \frac{1}{Z_P} & 0 \\ 0 & \frac{1}{Z_P} \end{bmatrix} \quad (12)$$

The values of the calculated inductances are plotted on a graph as shown in Fig. 9. Then the line connecting the two points is drawn. The intercept of the line, L_0 , is the inductance of the series parasitic components of the contact pad because L_i is the only component of the pad when the line length is zero. L_0 can be calculated by Eq. (13).

$$L_0 = 2L_i - L_{2i} \quad (13)$$

In this case, the measurement data of two transmission lines are used. However, by using growing number of transmission lines in different length, the more accurate value of L_0 can be obtained. In that case, the line shown in Fig. 9 is drawn by the method of least squares.

The same procedure is applied to the resistance. The series parasitic components of the pad, Z_S , is defined by the following equation.

$$Z_S = \frac{1}{2} \cdot (R_0 + j\omega L_0) \quad (14)$$

The parasitic components, Z_S and Z_P , can be obtained by Eq. (14) and Eq. (10). This pad model can be utilized for the de-embedding of other-DUTs.

IV. EXPERIMENTAL RESULTS

The evaluations of the conventional and proposed methods are applied by using the measurement data of transmission lines with different length. The structure of transmission lines is a coplanar strip line with a bottom ground as shown in Fig. 10. After de-embedding, the characteristic impedance Z_0 is calculated from S-parameter by Eq. (15). Fig. 11 shows

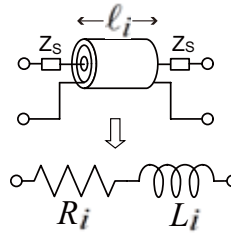


Fig. 8. The resistance and inductance of \mathbf{Y}_{X5} .

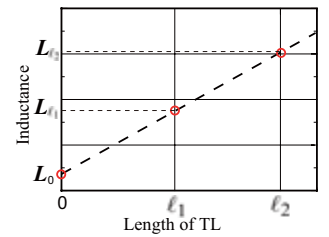


Fig. 9. The graph of the inductances.

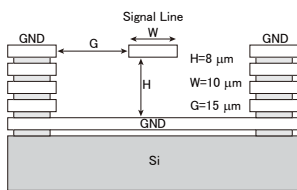


Fig. 10. The structure of TL.

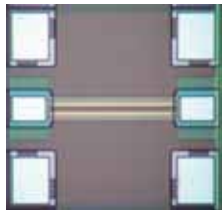


Fig. 11. The chip micrograph of TL.

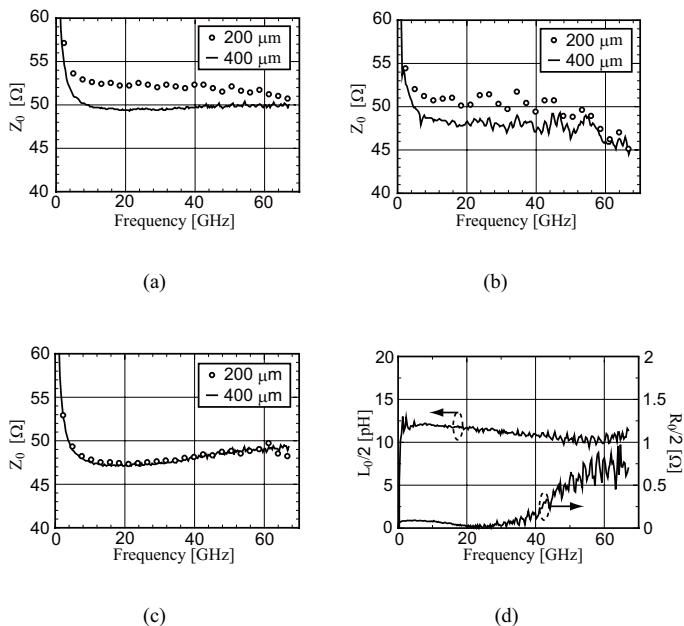


Fig. 12. The calculated result. (a) Open-Short. (b) Thru-only. (c) Proposed. (d) Z_S calculated by the proposed method.

the chip micrograph of the transmission lines with the contact pads.

$$Z_0^2 = Z_{nom}^2 \frac{(1 + S_{11})^2 - S_{21}^2}{(1 - S_{11})^2 - S_{21}^2} \quad (15)$$

where Z_{nom} represents the normalized impedance, and it is 50Ω in this case.

Fig. 12 shows the calculated results by the proposed and conventional methods. Fig. 12 (a) shows characteristic impedances of $200 \mu\text{m}$ -long and $400 \mu\text{m}$ -long transmission lines, which are de-embedded by the open-short method. Fig. 12 (b) shows a result by the thru-only method, and Fig. 12 (c) shows a result by the proposed method.

The characteristic impedance should be equal to each other even if it is calculated from different-length transmission lines. However, the open-short method and thru-only method have large error in characteristic impedance, which is caused by the error in the de-embedding calculation.

Using the proposed method, the characteristic impedances of the transmission lines agree with each other as shown in

Fig. 12 (c). This result demonstrates the accuracy of the proposed de-embedding method. The values of the series parasitic components Z_S are shown in Fig. 12 (d). The inductance of the series parasitic component is about 10 pH , and the resistance is less than 1Ω .

V. CONCLUSION

A new de-embedding method using two long lines is proposed. Using this method, the accurate de-embedding is realized, and it can be applied to transistors, capacitors, etc as well as transmission lines. The proposed de-embedding method is accurate even at mm-wave frequencies because it does not utilize the open- and short-patterns and the short thru pattern used in the conventional methods. The conventional dummy patterns cause the de-embedding error at mm-wave frequencies. The de-embedding of the transmission lines is demonstrated. In the experimental results, the error in characteristic impedance between the different-length transmission lines is less than 1Ω for the proposed method while two conventional methods have larger error.

ACKNOWLEDGEMENT

This work was supported by MIC, VLSI Design and Education Center (VDEC), the University of Tokyo in collaboration with Cadence Design Systems and Agilent Technologies Japan, Ltd. and Fujitsu Laboratories Ltd., Japan.

REFERENCES

- [1] A. Parsa and B. Razavi, "A 60GHz CMOS receiver using a 30GHz LO," in *IEEE International Solid-State Circuits Conference Digest of Technical Papers*, Feb. 2008, pp. 190–606.
- [2] J. F. Buckwalter and J. Kim, "A 26dB-Gain 100GHz Si/SiGe cascaded Constructive-Wave amplifier," in *IEEE International Solid-State Circuits Conference Digest of Technical Papers*, Feb. 2009, pp. 488–489.
- [3] Y. Hamada, M. Tanomura, M. Ito, and K. Maruhashi, "A high gain 77GHz power amplifier operating at 0.7V based on 90nm CMOS technology," *IEEE Microwave and Wireless Components Letters*, vol. 19, no. 5, May 2009.
- [4] P. J. V. Wijnjen, H. R. Claessen, and E. A. Wolsheimer, "A new straightforward calibration and correction procedure for "on-wafer" high frequency s-parameter measurements (45MHz-18GHz)," in *Proceedings of the Bipolar/BiCMOS Circuits and Technology Meeting*, Sep. 1987, pp. 70–73.
- [5] L. F. Tiemeijer, R. J. Havens, A. B. M. Jansman, and Y. Boutte-ment, "Comparison of the "Pad-Open-Short" and "Open-Short-Load" deembedding techniques for accurate On-Wafer RF characterization of High-Quality passives," *IEEE Transactions on Microwave Theory and Techniques*, vol. 53, no. 2, Feb. 2005.
- [6] M. Koolen, J. Geelen, and M. Versleijen, "An improved de-embedding technique for on-wafer high-frequency characterization," in *Proceedings of the Bipolar/BiCMOS Circuits and Technology Meeting*, Sep. 1991, pp. 188–191.
- [7] H. Ito and K. Masu, "A simple through only μ de embedding method for on wafer s parameter measurements up to 110 GHz," in *IEEE MTT-S International Microwave Symposium Digest*, June. 2008, pp. 383–386.
- [8] A. M. Mangan, S. P. Voinigescu, M.-T. Yang, and M. Tazlauanu, "De-embedding transmission line measurements for accurate modeling of IC designs," *IEEE Transactions on Electron Devices*, vol. 53, no. 2, Feb 2006.
- [9] J. Song, F. Ling, G. Flynn, W. Blood, and E. Demircan, "A de-embedding technique for interconnects," in *Electrical Performance of Electronic Packaging*, Oct. 2001, pp. 129–132.